



ELSEVIER

Contents lists available at SciVerse ScienceDirect

Ocean Engineering

journal homepage: www.elsevier.com/locate/oceaneng

Drag forces caused by submarine glide block or out-runner block impact on suspended (free-span) pipelines

Arash Zakeri^{a,*}, Bipul Hawlader^b, Ken Chi^{a,b}

^a C-CORE, Capitan Robert A. Bartlett Building, Morrissey Road, St. John's, NL A1B 3X5, Canada

^b Memorial University of Newfoundland, St. John's, NL A1B 3X5, Canada

ARTICLE INFO

Article history:

Received 14 April 2011

Accepted 17 March 2012

Editor-in-Chief: A.I. Incecik

Keywords:

Submarine glide block

Submarine out-runner block

Impact

Pipeline

Drag force

Centrifuge modeling

ABSTRACT

The results of a series of physical experiments to quantify the drag force on a submarine pipeline caused by a glide block or an out-runner block impact normal to the pipe axis are presented. The experiments were conducted in a geotechnical centrifuge under submerged conditions at a centrifugal force of 30 times the Earth's gravity (i.e. $N=30$) and simulated impact situations under steady state conditions and uniform velocities. The soil blocks (approximately 4.5 m high in prototype terms) were made of kaolin clay with undrained shear strengths between 4 and 8 kPa. The model pipes were 6.35 and 9.52 mm in diameter (0.19 and 0.29 m in prototype terms). The impact velocities ranged between 0.04 and 1.3 m/s. The pipe centerline was at mid-height of the block. The shear strain rates, defined as the ratio of impact velocity to pipe diameter. The shear strain rates ranged from about 4 to 137 reciprocal seconds. Hence, the test results are applicable to a wide range of field situations. A method is presented for estimating glide or out-runner block impact drag force on submarine pipelines based on the results of the centrifuge experiments.

© 2012 Elsevier Ltd. All rights reserved.

1. Introduction

Submarine landslides and the associated mass movement can potentially have devastating consequences on seafloor installations such as pipelines, flow lines, well systems, cables, etc. Submarine landslides occur frequently on both passive and active continental margins and slopes, releasing sediment volumes that may travel distances as long as hundreds of kilometers on gentle slopes (0.5 to 3°) over the course of less than an hour to several days (Nadim and Locat, 2005). The movement of landslide and the released sediment volumes are often called 'density flows'. From the initiation to deposition, density flows undergo complex processes that depend on many factors such as the composition, strength characteristics and properties, terrain topography, etc.

In an offshore oil and gas context geohazards can be presented by local and/or regional site and soil conditions having the potential to develop into failure events causing loss of life or damage to the environment and/or field installations. Triggering of these events can be caused by natural geological processes or by human activities, as outlined in a recent state-of-the-art review (Zakeri, 2009c). Research to understand the mechanisms behind and the risks posed by submarine landslides has intensified in the

past decade (e.g. De Blasio et al., 2004; Gauer et al., 2006; Norem et al., 1990; Zakeri et al., 2009c), mainly because of the increasing number of deep-water petroleum fields that have been discovered and, in some cases, developed. Production from offshore fields in areas with earlier sliding activities are ongoing in the Norwegian margin, Gulf of Mexico, offshore Brazil, the Caspian Sea and West Africa (Nadim and Locat, 2005).

Estimating magnitude of drag forces on pipelines caused by density flow impact is an important design consideration in the offshore engineering. For buried pipelines in cohesive soils in slowly moving unstable slopes, the available methods seem to provide more or less similar estimates for the drag force normal to the pipe axis. However, this is not the case for estimates of the longitudinal drag force (Zakeri, 2009c). In cohesive soils, the magnitude of the drag force is a function of the rate at which the soil is sheared during interaction with the pipe. Recent work by Zakeri et al. (2009a, 2008, 2009b) provide a method for estimating drag forces caused by a clay-rich debris flow (fully remolded and fluidized density flow—see Section 2 for the terminologies and definitions adopted in this paper) impacting a pipeline normal to its axis. Later, the work was extended to cover all angles of impact (Zakeri, 2009d).

This paper deals with quantifying the drag force resulting from impact of glide blocks or out-runner blocks on submarine pipelines at an angle normal to its axis. It is based on a series of physical tests carried out in a geotechnical centrifuge at C-CORE under submerged

* Corresponding author. Tel.: +1 709 864 4313; fax: +1 709 864 4706.
E-mail address: arash.zakeri@c-core.ca (A. Zakeri).

conditions at a centrifugal force of 30 times the Earth's gravity. The tests simulated an approximately 12 m long, 6 m wide and 4.5 m high intact glide block or out-runner block, with undrained shear strengths ranged between 4 and 8 kPa, impacting a submarine pipeline at velocities ranging between 0.04 and 1.30 m/s at mid-height of the 100% kaolin clay block. The model pipes were 6.35 mm and 9.52 mm in diameter, which correspond to 0.19 and 0.29 m in prototype terms. The shear strain rates, defined as the ratio of impact velocity to pipe diameter, ranged between about 4 and 137 reciprocal seconds. It should be noted that shear rate in a centrifuge model is N (i.e. the scaling factor) times higher than that in the prototype. As such, the test results are applicable to a wide range of field impact situations. For example, the shear strain rate resulting from a glide-block traveling at a velocity of 15 m/s impacting a 0.15 m diameter flowline would be 100 s^{-1} , which falls within the shear strain rates used in this study. Further, this paper adopts a geotechnical approach and presents a method for estimating glide block or out-runner block impact drag force on submarine pipelines based on the results from the centrifuge experiments.

2. Terminology and definitions

Submarine density flows are important sediment-transporting mechanisms and play a major role in the construction of deep-sea fans and deltas. Their triggering mechanisms, flow dynamics, interaction with the ambient water, depositional processes and consequences of failures have been studied by many researchers. The complexity of the flow from initiation to depositional processes associated with subaqueous density flows, combined with post-depositional consolidation and soft-sediment deformation, often make it difficult to interpret the characteristics of the original flow from the sedimentary record and therefore, to appropriately create models to address engineering problems. This has led to considerable confusion of nomenclature in the literature. Mulder and Alexander (2001) provide a simple yet comprehensive and encompassing classification of sedimentary density flows, based on physical flow properties and grain-support mechanisms, and briefly discuss the likely characteristics of the deposited sediments. The authors have followed their classification system with some modification in this paper. The terms used in this paper are defined as follows.

- **Glide block:** an intact hydroplaning block of cohesive sediment during early stages of density flow that has not been disintegrated and/or remolded. It still carries the strength properties of the parent sliding soil mass.
- **Out-runner block:** an intact block of cohesive sediment that has departed from the parent density flow during due to hydroplaning and rides freely downstream. It has not been remolded and still carries the strength properties of the parent landslide.
- **Debris flow:** a cohesive (clay-rich) flow with a minimum sediment concentration of 50% by volume that is fully remolded and fluidized. It can be characterized by rheological models for non-Newtonian fluids (e.g. Bingham, Herschel–Bulkley models). Its velocity profile consists of a uniform plug flow over a shear layer at the base.

3. Background information

Submarine landslides gained more interest after the Hurricane Camille event in August 1969. Camille struck the Gulf of Mexico, and damaged three platforms near its path. One platform was

found on its side on the bottom and the other two were abandoned because of large displacement. Later investigations concluded that significant sediment movements along the bottom were the main cause (Schapery and Dunlap, 1978). More recently, Hurricane Ivan in 2004 and Katrina in 2005 also generated sediment movements and damaged pipelines in the Gulf of Mexico (Nodine et al., 2007).

A number of techniques have been proposed to assess the drag forces arising from pipeline–density flow interaction including the situations encompassing onset of a landslide. The problem has been investigated from two perspectives: a geotechnical approach and a fluid dynamics approach. In the former, the drag forces are directly linked to the soil shear strength, either linearly or through a power–law relationship including the rate of shear. The latter approach considers the density flow as fully fluidized and applies fluid dynamics and rheology principles of a non-Newtonian fluid flow (Zakeri, 2009c).

In the geotechnical approach, the drag force per unit length of pipeline, F_D , is estimated from the following general form of equation:

$$F_D = k s_u D \quad (1)$$

where k is the model parameter (a constant or shear strain rate dependent), s_u is the undrained shear strength of the soil and D is the pipe diameter. Demars (1978), Swanson and Jones (1982), Bea and Aurora (1982), Audibert et al. (1984), and Summers and Nyman (1985) all adopted the geotechnical approach, with the k parameter being a constant, to study drag forces on buried pipelines in an unstable clay-rich slope. Georgiadis (1991) investigated the strain-rate dependency of the drag force on a pipeline embedded in a moving clay-rich soil mass and modified the conventional geotechnical approach (i.e. the k parameter being a function of strain rate). Calvetti et al. (2004) adopted the geotechnical approach for pipelines in unstable sand-rich slopes.

In the fluid dynamics approach, the drag force per unit length of a pipeline is estimated from the following equation:

$$F_D = \frac{1}{2} \rho C_D U_\infty^2 D \quad (2)$$

where ρ is the density of the density flow, C_D is the drag coefficient and U_∞ is the free upstream velocity (e.g. Chhata et al., 2003; Pfeiff and Hopfinger, 1986).

Zakeri et al. (2008) adopted the fluid dynamics approach to estimate the drag forces on suspended and laid-on-seafloor pipelines. In that work a slurry mixture of kaolin clay, silica sand, water and black diamond coal slag (for visual purposes) was used to simulate the debris flow impact. Attack angles ranging between 90° (normal) and 0° (longitudinal), were also investigated (Zakeri, 2009a, b, d; Zakeri et al., 2009a). For debris flows, the following relationship has been proposed for estimating the drag force coefficient for drag forces normal to the pipe axis for impacts at various angles:

$$C_{D-90} = 1.4 + \frac{17.5}{\text{Re}_{\text{non-Newtonian}}^{1.25}} \quad (3)$$

In the above equation, $\text{Re}_{\text{non-Newtonian}}$ is defined by $\rho U_\infty^2 / \tau$, where τ is the fluid shear stress at a certain shear strain rate (defined by Eq. (4)) caused by pipe–debris flow interaction upon impact.

$$\dot{\gamma} = \frac{U_\infty}{D} \quad (4)$$

Within reasonable agreement, the aforementioned geotechnical approaches are only applied to the case of buried and partially buried pipelines installed in unstable slopes. Integrated geotechnical and geophysical site investigations have indicated that debrites (i.e. deposits of debris flows) are homogenous and rather

uniform in characteristics (e.g. Jeanjean et al., 2006). Hence, the fluid dynamics approach may be more applicable to the case of debris flow impact on pipelines where the moving soil mass has been fully remolded and fluidized by entraining ambient fluid and soft seabed sediments along the path. However, there is need to develop a method to estimate drag force caused by glide block or out-runner block impact on pipelines.

4. Model scaling considerations

The geotechnical centrifuge is useful for scale modeling of any large-scale nonlinear problem for which gravity is a primary driving force. Centrifuge modeling of geotechnical problems is a well-established method. The procedures and appropriate scaling laws for geotechnical centrifuge modeling have been given by Taylor (1995) and Garnier et al. (2007). Geotechnical materials have nonlinear mechanical properties that depend on the effective stress and stress history. The centrifuge applies an increased “gravitational” acceleration to physical models in order to produce identical self-weight stresses in the model and prototype. The one to one scaling of stress enhances the similarity of geotechnical models and makes it possible to obtain accurate data to help solve complex problems such as earthquake-induced liquefaction and soil-structure interaction. Centrifuge model testing provides data to improve our understanding of basic mechanisms of deformation and failure, and provides benchmarks useful for verification of numerical models.

For modeling of glide blocks or out-runner blocks, which are essentially intact sections of a failed slope of cohesive material, one need to reproduce the correct stress level within the soil mass to ensure that the undrained shear strength of the soil, which depends on the effective stress level, is similar to that of prototype situations. Further, such blocks have dimensions that are in the order of meters. Hence, the use of centrifuge modeling techniques becomes necessary where a large-scale geotechnical process can properly be scaled down using appropriate scaling laws while maintaining proportionality between the prototype and model parameters such as dimensions, shear rate, strength properties, pore pressure diffusion (e.g. consolidation), heat conduction, etc. Undrained shear strengths ranging between 4 and 20 kPa are typically observed within the upper 10 m of seabed profiles. Undrained shear strength is a function of soil effective stress and stress history. Shear strength profiles similar to prototype situations can be reproduced in the centrifuge.

Essentially, any small- or reduced-scale modeling of this phenomenon in a controlled environment should be capable of simulating large dimensions while maintaining correct stress characteristics and undrained conditions during the interaction between the block and the pipe. Table 1 summarizes the general scaling factors adopted for centrifuge testing. Appendix A briefly describes principles and scale effects in centrifuge modeling. To model subaqueous conditions, the tests were carried out under

submerged conditions. This is important as the entrapped water in the wake behind the pipe plays a role in the magnitude of the drag force. It is also important to consider the difference in the time scaling factors for dynamic events and diffusion (consolidation and seepage). Garnier et al. (2007) assess the transition between partially drained and fully undrained behavior through the normalized velocity ($V_{Normalized}$) defined by:

$$V_{Normalized} = \frac{\dot{U}d}{c_v} \tag{5}$$

where \dot{U} is the penetration rate, d is its diameter and c_v is the coefficient of consolidation of the clay. For typical normally consolidated kaolin clay, the transition values are respectively $V_{Normalized}=0.01$ (fully drained) and $V_{Normalized}=30$ (fully undrained). For the test results presented in this paper, the clay behavior around the pipe is fully undrained given the impact velocities.

The shear strain rate (given by Eq. (4)) in the centrifuge model—is N times higher than that in the prototype. In the current study, the shear strain rate for the soil-pipe interaction is also defined by Eq. (4), where U_∞ is the glide block or out-runner block impact velocity. Dimensional analysis based on Buckingham's Pi Theorem (Buckingham, 1915) indicates that the physical variables for this problem are: pipe diameter, impact velocity, undrained shear strength and submerged unit weight of the block. The latter does not change significantly in both model and prototype situations. The Reynolds number from interaction of the block with the ambient water is high—greater than 10^5 . The hydrodynamic resistance provided by the inertial drag of the ambient water is irrelevant to this study given the setup as described below. However, it is important to conduct the tests under submerged conditions as the water entrapped in the wake behind the pipe plays a role in the overall drag force.

5. Experimental setup

Fig. 1 illustrates the experimental setup; the dimensions provided are in model terms, unless specified. The tests were conducted in a 1260 mm × 640 mm × 1020 mm ($L \times H \times W$) aluminum strongbox. In the middle of the box were two 1000 mm long, 11.3 mm wide and 300 mm high plexiglass walls placed at 200 mm apart. The space between the plexiglass walls essentially formed a flume and is referred to as ‘the flume’ in this paper. Inside the flume, there was an L-shaped aluminum cart on which the clay block (400 mm long, 200 mm wide and approximately 150 mm high) was placed. A geotextile was placed on the base of the cart to promote bottom drainage during the in-flight consolidation phase. The clay block was constrained by the back of the cart, two plexiglass walls to the side, and another 11.3 mm thick plexiglass gate at the front. The influence of plexiglass on the movement of clay was considered insignificant (i.e. slip-free boundary conditions or minimal boundary effect Crowe et al. (2001). The gate was placed in a 12 mm groove made in the plexiglass walls. Beneath the cart were four linear bearings sitting on top of two linear precision shafts. The front of the cart was connected by a 2.4 mm aircraft cable through a pulley to a servomotor that almost instantaneously accelerates the cart to impact velocities as high as 1.3 m/s. A string potentiometer was connected at the back of the cart to measure the distance traveled, so that velocity can be back-calculated.

The model pipe was located 220 mm in front of the cart. Two stainless steel model pipes with outer diameters of 6.35 mm and 9.52 mm were used, which correspond to prototype pipe diameters of 0.19 m and 0.29 m respectively, given the scaling factor of 30 in the experiments. The vertical location of the pipe was

Table 1
General scaling factors for centrifuge tests.

Physical property	Unit	Model scale
Gravitation acceleration	LT ⁻²	N
Dimension—length and diameter	L	1/N
Stress	ML ⁻¹ T ⁻²	1
Force	MLT ⁻²	1/N ²
Velocity	LT ⁻¹	1
Time—dynamic events	T	1/N
Time—consolidation and seepage	T	1/N ²
Strain	–	1
Shear strain rate	T ⁻¹	N

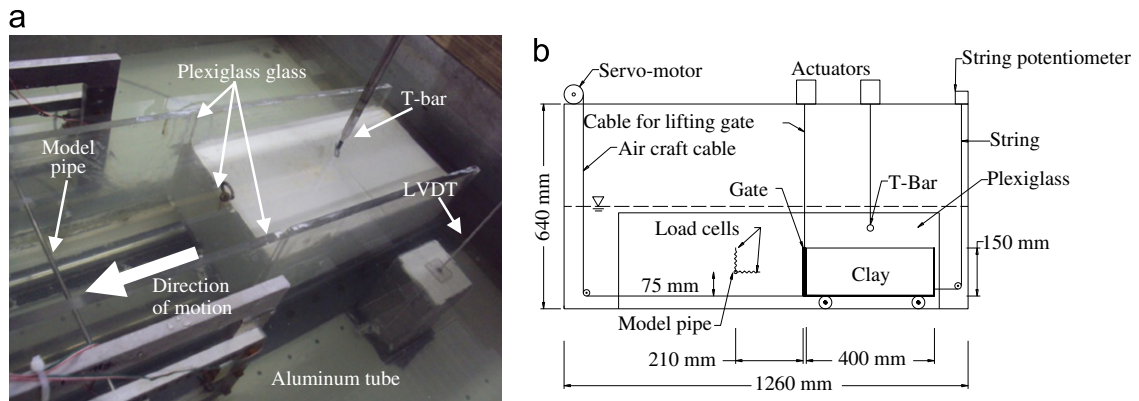


Fig. 1. Experimental setup. (a) Clay block placed on the L-shaped cart ready for testing. (b) Setup elevation view with dimensions.

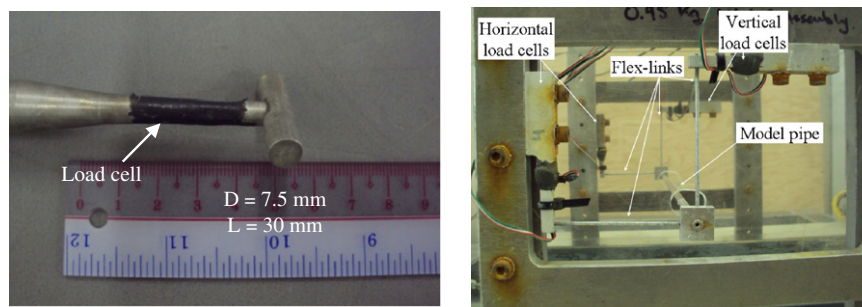


Fig. 2. T-bar (left) to measure undrained shear strength and load cell system (right) for measuring the impact drag force in the vertical and horizontal directions.

75 mm above the base of the cart, adjustable to ensure that the impacts occur at mid-height of the clay block; hence, the crown and bottom of the largest pipe have at least 4.5 times the diameter distance from the top and base of the clay. The model pipe was extended through the plexiglass wall on both sides via a 20 mm hole and were connected to two sets of vertical and horizontal load cells (see Fig. 2). Both the ends of the pipe were fitted through the pipe mounts. Each pipe mount was connected to two load cells by two 3 mm diameter solid aluminum rods, essentially forming flex-links. Proper calibration of the load cells was carried out following the fabrication and periodically throughout the program. The flex-links caused no cross-communication between the horizontal and vertical load cells.

There was a need to monitor the clay consolidation during the flight. Linear Variable Differential Transformers (LVDTs) and Pore Pressure Transducers (PPTs) are typically used to monitor clay consolidation in the centrifuge. It was impossible to place LVDTs on and PPTs in the clay block, given that its movement would damage the instruments. Therefore, a separate sample of the same clay was prepared for consolidation monitoring purposes. For that purpose, an aluminum box, 80 mm × 80 mm in cross-section and 200 mm in height, was placed outside the flume to facilitate monitoring of clay consolidation during the flight. The aluminum tube (1.6 mm wall thickness) contained the same consolidated clay sample as the block. A layer of geotextile was placed at the base of the clay and then filled with a layer of sand for drainage and to elevate the clay surface in the box to the elevation of the clay block. To monitor centrifuge consolidation, a LVDT was placed on top of the clay and two PPTs were installed in the middle of the clay.

Above the cart were two actuators supported by two I-beams. The two actuators were used to conduct undrained shear strength testing using a T-bar (Stewart and Randolph, 1994) and to lift the plexiglass gate. The T-bar (Fig. 2) apparatus used in these experiments was

7.5 mm in diameter and 30 mm in length. The T-bar tests were conducted to obtain the intact and remolded undrained shear strengths at a penetration rate of 3 mm/s, ensuring penetration was in an undrained condition (Oliviera and Almeida, 2010; Stewart and Randolph, 1994).

6. Sample preparation and centrifuge testing procedures

The soil used in this study was 100% kaolin clay consolidated from a slurry state to the desired consolidation stress in the laboratory. The geotechnical properties of the kaolin clay are: Liquid Limit (LL)=60%, Plastic Limit (PL)=32% and Specific Gravity (G_s)=2.6. The kaolin clay slurry was mixed under vacuum condition at water content of 120%, which is equal to 200% of LL . The slurry was then transferred into a 900 mm long, 450 mm high and 300 mm wide box for lab-floor consolidation. At the base of the consolidation box, there were perforated steel plates (398 mm × 198 mm) above the geotextile and sand drainage layer. These plates facilitated trimming of the clay sample and transferring it onto the cart with minimal disturbance. The slurry was allowed to consolidate under 4 kPa (stress generated from the piston plate) consolidation pressure for 24 h. The progress of consolidation was monitored using Taylor's square-root-of-time method (\sqrt{t} -method). After well past 90% of consolidation, a step-load was applied from the top and the clay was again allowed to consolidate under that applied load. The final lab-floor consolidation pressures ranged between 40 and 120 kPa.

Following termination of the lab-floor consolidation, the clay block was cut from the consolidated clay, trimmed to the desired dimensions and placed on the aluminum cart over a layer of geotextile for centrifuge testing. Another small block of clay (80 mm × 80 mm, the same height as the clay block) used to monitor centrifuge consolidation (see Fig. 1a) was prepared by

penetrating the aluminum tube into the consolidated clay. The centrifuge consolidation was monitored by an LVDT placed on top of the clay in the aluminum tube and using two PPTs.

In the strongbox, the sides of the clay block were supported by the cart and the plexiglass. During the centrifuge test at 30 g, the clay was allowed to consolidate under self weight. The resulting heights of the clay blocks ranged between 140 mm and 160 mm. Consolidation time of the sample ranged between two to three hours. After completion of consolidation in the centrifuge, T-bar testing was conducted on the clay block sample located on the cart to determine its intact and remolded undrained shear strength. After the T-bar test, the plexiglass gate was raised and the servo-motor pulled the cart towards the model pipe, impacting the model pipe at the mid-height of the clay block. The recorded data for the T-Bar tests was 40 Hz; impact test data ranged from 400 to 2000 Hz. All tests were conducted under submerged conditions. Fresh water was used to prepare the clay samples as well as in the centrifuge tests.

It should be noted that upon lifting the gate, a portion of the front face of the clay failed due to the increased shear stress locally imposed on the sample by the removal of support. The failure pattern is similar to undrained failure of a vertical cut with a slope of approximately 45°. The test setup was designed to allow this failed material to flow under the cart and to have no influence on the test results.

7. Experiment results, analysis and discussion

A total of eleven (11) tests were conducted at 30 g, varying undrained shear strengths of soil, pipe diameters and impact velocities. Table 2 summarizes of the test conditions and the results. The following sections discuss the analysis and interpretations of the results.

7.1. Undrained shear strengths

Following completion of the in-flight consolidation, a T-bar penetrometer was used to assess the intact and remolded undrained shear strength (s_u) profile in the clay block. The undrained shear strength was calculated by using the following equation:

$$s_u = \frac{P}{N_b d} \tag{6}$$

where P is force per unit length on the T-bar, d is the diameter of the T-bar and N_b is a T-bar factor. In this study, $N_b=10.5$ was used

(Stewart and Randolph, 1994). The T-bar results were corrected for the buoyancy effect of water. The remolded undrained shear strength was assessed by cycling the T-bar up and down until the values of the penetrometer resistance reached a steady value. This typically occurred after 5 cycles. Due to technical problems, the T-bar data for Tests 4 and 5 were not recorded; however, since the final consolidation stress was the same, the shear strengths were estimated from Test 1. Fig. 3 illustrates that undrained shear strength profiles measured. The moisture contents, which were taken from the undisturbed clay located in the aluminum tube after completion of the centrifuge tests, were between 60 and 75%.

7.2. Force–displacement relationship

Figs. 4 and 5, respectively, illustrate the horizontal and vertical drag forces measured in the physical experiments as the pipe penetrates into the clay block. In all the experiments, a small wedge of the clay face failed upon opening of the gate. The effect of this is evident in both horizontal and vertical forces within approximately the first 75 mm of penetration. Beyond this distance the steady-state drag force is reached very quickly. Fig. 6 presents an example of test results obtained from Test 7. The servo-motor system it made possible to almost instantaneously reach and maintain the test velocity. The initial uplift of the pipes within about the first 50 mm of horizontal displacement (Fig. 5) is mainly due to a failed wedge in front of the block. This uplift diminishes as

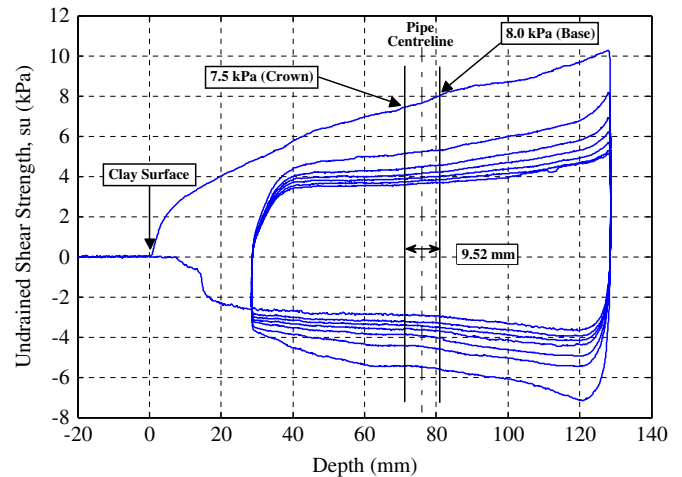


Fig. 3. Undrained shear strength profiles of Test 10 (displacement in model terms).

Table 2
Summary of the experiment conditions and results in model terms.

Test no.	Impact velocity (m/s)	Clay height (mm)	Pipe diam. (mm)	Depth to middle of pipe (mm)	Consolidation pressure (kPa)	Shear strengths at pipe— s_u (kPa)		Horizontal drag force per unit length, F_D (N/m)	Shear strain rate (1/s)	k -parameter
						Intact	Remolded			
1	0.16	156	6.35	81	40	4.3	1.4	327	24.5	12.0
2	0.21	142	6.35	67	60	4.7	2.0	333	32.8	11.2
3	0.10	144	6.35	69	60	4.4	2.0	297	16.5	10.8
4	0.10	160	9.52	85	40	4.1**	1.4	385	10.8	9.9
5	0.20	160	9.52	85	40	4.1**	1.4	383	21.4	9.9
6	1.30	140	9.52	65	80	4.4	2.1	609	136.6	14.7
7	0.77	142	9.52	67	100	6.0	2.4	729	81.4	12.8
8	0.30	144	6.35	69	100	6.7	4.3	484	47.8	11.3
9	0.20	151	6.35	76	120	7.5	3.7	490	32.1	10.2
10	0.10	141	6.35	66	120	8.0	4.5	522	16.2	10.3
11	0.04	151	9.52	76	120	7.8	3.7	687	4.3	9.3

* The values reported represent average measured intact and remolded undrained shear strengths at the vertical location immediately above and below the model pipe.

** The undrained shear strength for Tests 4 and 5 were estimated from Test 1 shear strength profile.

the pipe penetrates into the block. Oliveira et al. (2010) demonstrated in physical modeling, by moving a pipe through a 80% kaolin and 20% smectite clay at different h/D (height/ diameter) ratios, that when h/D is greater than 1, the vertical forces become negligible. In the experiments conducted, the h/D ratio ranged from 6.8 to 12.8 and the magnitude of the upward vertical forces were insignificant compared to the horizontal forces.

7.3. Analysis of the horizontal drag force

Drag force is rate dependent. The geotechnical approach was adopted to analyze the test results. This is appropriate for the case of glide or out-runner block impact on pipelines. Table 2 summarizes the analysis results. The drag forces used in the analyses are the maximum values determined at steady-state conditions. Eq. (1) was used to calculate the k -parameter for each test. Fig. 7 plots the calculated k -parameter values against the shear strain rates estimated by Eq. (4). The fit to the physical test data can be described by the following equation:

$$k = 7.5 \times \dot{\gamma}^{0.12} \quad (7)$$

where $\dot{\gamma}$ is in reciprocal seconds. The R-squared value for the fit is 0.79. Eq. (7) is directly applicable to prototype situations. This relationship is proposed for estimating the drag force normal to the pipe axis caused by glide or out-runner block impact on a submarine pipeline within the shear strain rates tested. One may choose to utilize numerical methods to further populate the data and extend it beyond the limits tested. Also more physical and

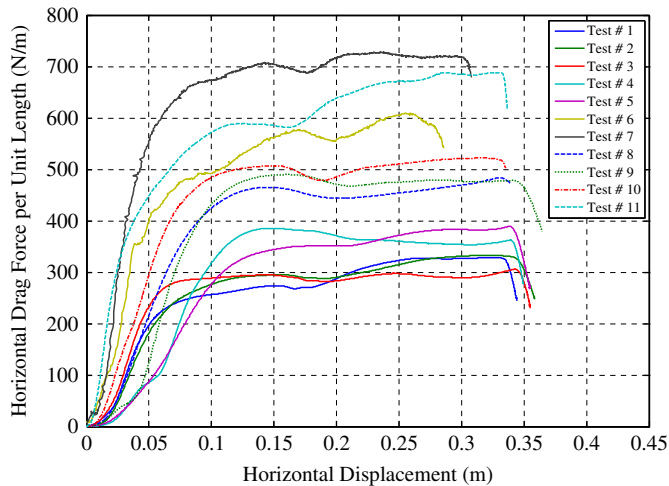


Fig. 4. Horizontal drag force of the experiments (model terms).

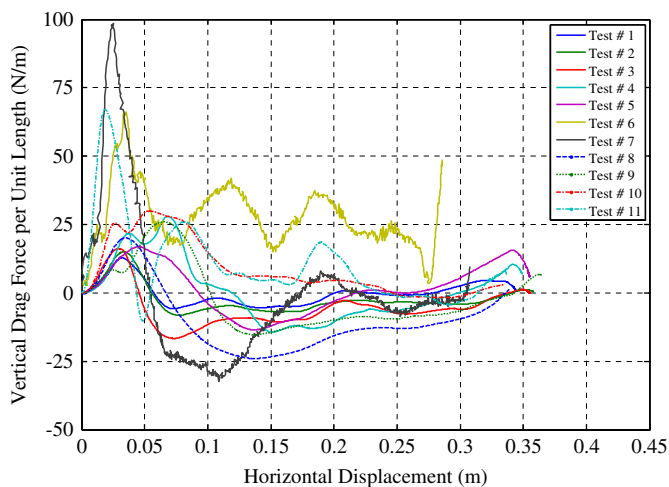


Fig. 5. Vertical drag force of the experiments (model terms).

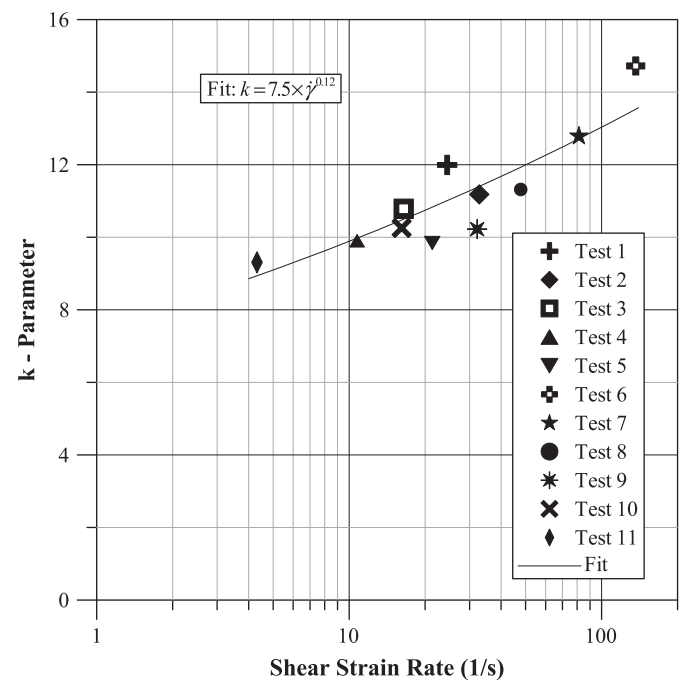


Fig. 7. Shear strain rate versus model parameter, k , for model or prototype terms.

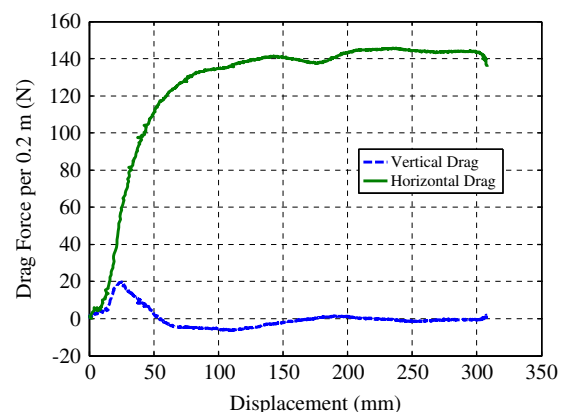
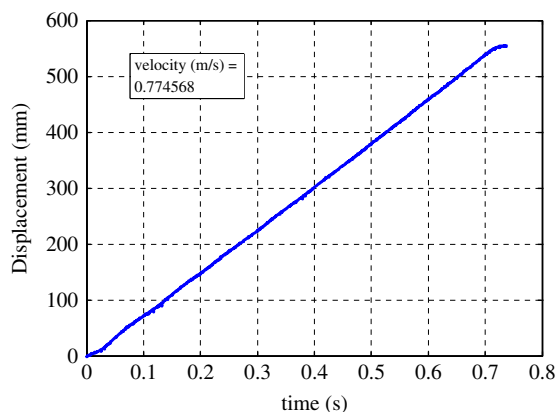


Fig. 6. Example test results—velocity and drag forces from Test no. 7.

numerical experiments are required to investigate the drag forces, normal and longitudinal, for various impact angles.

8. Numerical example of impact drag force estimation

Consider a 100 m section of a 0.15 m diameter suspended (free-span) pipeline that is subjected to impact by a submarine glide block (having a density of 1600 kg/m³ and average undrained shear strength of 5 kPa at pipeline location) approaching at 3 m/s. The impact is normal to the pipe axis. The shear strain rate is:

$$\dot{\gamma} = \frac{U_{\infty}}{D} = \frac{3}{0.15} = 20(\text{s}^{-1})$$

The k -parameter is:

$$k = 7.5 \times 20^{0.12} = 10.75$$

Using Eq. (1), one obtains the impact drag force in kN/m normal to the pipe axis as per below:

$$F_D = k \times s_u \times D = 10.75 \times 5 \times 0.15 = 8.06(\text{kN/m})$$

It is assumed that the pipeline is moored to the seafloor and does not deform or move when hit by the glide block.

9. Conclusions

A new experimental setup was developed for modeling drag force caused by glide block or out-runner block impact on offshore suspended pipelines. A series of centrifuge tests were successfully conducted using this experimental setup. The experimental setup performed very satisfactorily and proved to be quite efficient. The experiments verify that, for large debris blocks, impact forces on pipelines can be reliably determined. Impact velocity or undrained shear strain rate has been identified as one of the key parameters for modeling drag force. Tests were conducted under different shear strain rate, pipe diameter and undrained shear strength. The drag force can be estimated using a normalized k -parameter (Eq. (1)). Based on this experimental study, the following conclusions are drawn:

- It was found that drag force is rate dependent and varies according to power–law relationship as a function of shear strain rate as defined by Eq. (4). The drag force is in direct relationship with the undrained shear strength of the soil. It is logical to deduce that the undrained shear strength of a soil also varies with shear strain rate according to power–law relationship.
- In practice, submarine pipe diameters range between 0.1 m and 1.0 m. Assuming a glide-block or out-runner block velocity of between 1 m/s and 10 m/s, the shear strain rate upon the impact with a pipe would be in the range of 1 s⁻¹ to 100 s⁻¹. The experiments covered shear strain rates between 4 s⁻¹ and 137 s⁻¹ (i.e. about two log cycles), and therefore are considered appropriate for practical purposes.
- For design purposes, the k -parameter for estimating the normal drag force is $k = 7.5 \times \dot{\gamma}^{0.12}$. This model is based on a fit to physical test data and valid within the range tested. It is directly applicable to prototype situations. Given the scatter in the data, one may choose to allow for some factor of safety when applying this equation to prototype situations. Numerical modeling is recommended to further investigate the matter and to increase confidence in the model.
- Although the present study provides a method for quick and efficient estimation of drag force, the model is simply based on the experimental results presented above and is valid for impact situations normal to the pipeline axis. Confirmatory

and complementary physical testing and numerical modeling is recommended to investigate the drag forces, normal and longitudinal, for various impact angles.

It should be noted that the above model and test results are based on an intact block of soil impacting a pipe. This may be somewhat conservative as glide-blocks and out-runner blocks undergo some internal deformations as they travel downstream, which in turn, results in reduction in shear strength. Therefore, the model presented here is likely to provide an upper-bound estimate. Given some scatter in the data, numerical modeling can provide valuable insight and increase confidence in the model.

Acknowledgments

The presented work was supported by C-CORE which is greatly appreciated. We also express our sincere gratitude to Bradley Elliott, Gerry Piercey, Don Cameron, Karl Tuff and Derry Nicholl of the C-CORE Geotechnical Group for their significant efforts, help and contribution to this research program. We owe the success of this program to them. We also extend our gratitude to the reviewers for their contribution to this paper.

Appendix A. Principles and scale effects in centrifuge modeling

A geotechnical centrifuge is essentially a sophisticated load frame on which soil samples, soil-structure and fluid-soil-structure interaction phenomena can be tested. It is analogous to the wind tunnel for aeronautical engineers and the flume in hydraulic engineering. Taylor (1995) provides a detailed description of centrifuge modeling, principles and simulation of various geotechnical phenomena. This appendix is mainly excerpted from the Taylor (1995).

A special feature of geotechnical modeling is the necessity of producing the soil behavior in terms of both strength and stiffness. The soil behavior is a function of in-situ stress level and stress history that change with depth. A geotechnical centrifuge can correctly reproduce this. If the same soil is used in the model as the in the prototype, under careful preparation, and then subjected to an inertial acceleration field that is N times Earth's gravity the vertical stress at depth h_m will be identical to that in the corresponding prototype at depth h_p (i.e. $h_p = Nh_m$). This is the basic scaling law of centrifuge modeling. In other words, if an acceleration of N times Earth's gravity is applied to a material of density ρ , then the vertical stress σ_{vm} , at depth h_m in the model is given by $\sigma_{vm} = \rho N g h_m$, where g is the Earth's acceleration. The vertical stress in the prototype is $\sigma_{vp} = \rho g h_p$. Thus, for $\sigma_{vm} = \sigma_{vp}$, $h_m = h_p N^{-1}$, indicating that linear dimension is scaled 1: N (model:prototype). It follows that strains have a scale factor of 1:1; therefore, the part of the soil stress–strain curve mobilized in the model will be identical to the prototype.

Model displacements will be N times smaller than the prototype; therefore, the scale factor for velocity will be 1:1. Consolidation related to the dissipation of excess pore pressure. The degree of consolidation is described by the dimensionless time factor T_v defined as $T_v = c_v t / H^2$, where c_v is the coefficient of consolidation (an intrinsic property of soil), t is time and H is a distance related to the drainage path. For a model to have the same degree of consolidation as the prototype, $T_{vm} = T_{vp}$. Therefore, $c_{vm} t_m / H_m^2 = c_{vp} t_p / H_p^2$, if once used the same soil material, then $c_{vm} = c_{vp}$. Since, $H_p = N H_m$, then $t_m = (1/N^2) \cdot t_p$. Hence, the scale factor for time is 1: N^2 meaning that the consolidation time or dissipation of excess pore pressure in the centrifuge will be much shorter than the

prototype. For example, a consolidation event lasting 400 day in the prototype can be reproduced in one-hour centrifuge run at 100g. This scaling also applies to other diffusion events, such as heat transfer by conduction.

Two major considerations in centrifuge modeling are the scaling laws and scaling errors. Shear strength of clays is a function of stress history and stress level. Hence, the scaling factor for shear strength is 1:1. However, shear rate (defined as the ratio of velocity and a characteristics length) has a scaling factor of $N:1$ since linear dimension is scaled as $1:N$ and velocity scale is $1:1$. This means that shear rate in a centrifuge model is N times larger than that in the prototype. This requires careful attention as to properly modeling problems in a centrifuge and avoiding scaling issues. For modeling the interaction between the fast moving clay block and the pipe in a centrifuge, one needs to consider the scaling laws associated with both the rate of shearing and the rate of pore pressure dissipation. In prototype situations, this intersection is fast enough such that soil shearing takes place under undrained conditions. This issue was addressed via Eq. (5) for the series of tests conducted in this study.

References

- Audibert, J.M.E., Nyman, D.J., O'Rourke, T.D., 1984. Differential Ground Movement Effects on Buried Pipelines. In: Technical Council on Lifeline Earthquake Engineering (Ed.), Guidelines for the Seismic Design of Oil and Gas Pipeline Systems. American Society of Civil Engineers, pp. 150–183.
- Bea, R.G., Aurora, R., 1982. Design of Pipelines in Mudslide Areas, Proceedings of the 14th Annual Offshore Technology Conference (OTC), Huston, Texas, pp. 401–414.
- Buckingham, E., 1915. The principle of similitude. *Nature* 96 (2406), 396–397.
- Calvetti, F., di Prisco, C., Nova, R., 2004. Experimental and numerical analysis of soil–pipe interaction. *J. Geotech. Geoenviron. Eng.* 130 (12), 1292–1299.
- Chehata, D., Zenit, R., Wassgren, C.R., 2003. Dense granular flow around an immersed cylinder. *Phys. Fluids* 15 (6), 1622–1631.
- Crowe, C.T., Elger, D.F., Roberson, J.A., 2001. *Engineering Fluid Mechanics*. Wiley, New York.
- De Blasio, R., Elverhoi, A., Issler, D., Harbitz, C.B., Bryn, P., Lien, R., 2004. Flow models of natural debris flows originating from overconsolidated clay materials. *Mar. Geol.* 213 (1–4), 439–455.
- Demars, K.R., 1978. Design of marine pipelines for areas of unstable sediment. *Transp. Eng. J. ASCE* 104 (1), 109–112.
- Garnier, J., Gaudin, C., Springman, S.M., Culligan, P.J., Goodings, D., Konig, D., Kutter, B., Phillips, R., Randolph, M.F., Thorel, L., 2007. Catalogue of scaling laws and similitude questions in centrifuge modelling. *Int. J. Phy. Modell. Geotech.* 7 (3), 1–24.
- Gauer, P., Elverhoi, A., Issler, D., De Blasio, F.V., 2006. On numerical simulations of subaqueous slides: Back-calculations of laboratory experiments of clay-rich slides. *Norw. J. Geol.* 86 (3), 295–300.
- Georgiadis, M., 1991. Landslide drag forces on pipelines. *Soils Found* 31 (1), 156–161.
- Jeanjean, P., Berger, W.J., Liedtke, E.A., Lanier, D.L., 2006. Integrated Studies To Characterize the Mad Dog Spar Anchor Locations and Plan Their Installation, OTC 18004, Offshore Technology Conference (OTC), Houston, Texas, USA.
- Mulder, T., Alexander, J., 2001. The physical character of subaqueous sedimentary density flows and their deposits. *Sedimentology* 48 (2), 269–299.
- Nadim, F., Locat, J., 2005. Risk Assessment for Submarine Slides. In: Hunger, O., Fell, R., Couture, R., Eberhardt, E. (Eds.), *International Conference for Landslide Risk Management*. A.A. Balkema, Vancouver, BC, Canada, pp. 321–334.
- Nodine, M.C., Gilbert, R.B., Wright, S.G., Cheon, J.Y., Wrzyszczyński, M., Coyne, M., Ward, E.G., 2007. Impact of Hurricane-Induced Mudslides on Pipelines, Offshore Technology Conference (OTC), Houston, Texas, USA.
- Norem, H., Locat, J., Schieldrop, B., 1990. An approach to the physics and the modeling of submarine flowslides. *Mar. Geotech.* 9 (2), 93–111.
- Oliveira, J.R.M.S., Almeida, M.S.S., Almeida, M.C.F., Borges, R.G., 2010. Physical modeling of lateral clay–pipe interaction. *J. Geotech. Geoenviron. Eng.* 136 (7), 950–956.
- Oliveira, J.R.M.S., Almeida, M.S.S., 2010. Pore-pressure generation in cyclic T-bar tests on clayey soil. *Int. J. Phys. Modell. Geotech.* 10 (1), 19–24.
- Pfeiff, C.F., Hopfinger, E.J., 1986. Drag on cylinders moving through suspensions with high solid concentration. *Physicochem. Hydrodyn.* 7 (2–3), 101–109.
- Schapery, R.A., Dunlap, W.A., 1978. Prediction of Storm Induced Sea Bottom Movement and Platform Forces, Proceedings of the 10th Annual Offshore Technology Conference (OTC), Houston, Texas, pp. 1789–1796.
- Stewart, D.P., Randolph, M.F., 1994. T-Bar penetration testing in soft clay. *J. Geotech. Eng., ASCE* 120 (12), 6.
- Summers, P.B., Nyman, D.J., 1985. An approximate procedure for assessing the effects of mudslides on offshore pipelines. *J. Energ. Resour. Technol.—Trans. ASME* 107 (4), 426–432.
- Swanson, R.C., Jones, W.T., 1982. Mudslide effects on offshore pipelines. *Transp. Eng. J. ASCE* 108 (6), 585–600.
- Taylor, R.N., 1995. *Geotechnical Centrifuge Technology*. Blackie Academic & Professional, London.
- Zakeri, A., 2009a. Corrigendum to “Submarine debris flow impact on pipelines—Part II: numerical analysis”. *Coast. Eng.* 56 (1), 1.
- Zakeri, A., 2009b. Estimating Drag Forces on Suspended and Laid-on-Sea-floor Pipelines Caused by Clay-Rich Submarine Debris Flow Impact. In: D.M.e.a. (Ed.), *Submarine Mass Movements and Their Consequences*, 2009. Springer Science+Business Media B.V., Austin, Texas, USA, pp. 83–94.
- Zakeri, A., 2009c. Review of the state-of-the-art: drag forces on submarine pipelines and piles caused by landslide or debris flow impact. *J. Offshore Mech. Arctic Eng., Am. Soc. Mech. Eng. ASCE* 131 (1). <http://dx.doi.org/10.1115/1.1111.2957922>.
- Zakeri, A., 2009d. Submarine debris flow impact on suspended (free-span) pipelines: noraml and longitudinal drag forces. *Ocean Eng.* 36, 10.
- Zakeri, A., Hoeg, K., Nadim, F., 2009a. Submarine debris flow impact on pipelines: numerical modeling of drag forces for mitigation and control measures. *SPE Projects, Facilities Construction* 2009, 11.
- Zakeri, A., Hoeg, K., Nadim, F., 2008. Submarine debris flow impact on pipelines—Part I: experimental investigation. *Coast. Eng.* 55, 1209–1218.
- Zakeri, A., Hoeg, K., Nadim, F., 2009b. Submarine debris flow impact on pipelines—Part II: numerical analysis. *Coast. Eng.* 56, 1–10.
- Zakeri, A., Si, G., Marr, J.D.G., Hoeg, K., 2009c. Experimental Investigation of Subaqueous Clay-Rich Flows, Generated Turbidity and Sediment Deposition. In: D.M.e.a. (Ed.), *Submarine Mass Movements and Their Consequences*, 2009. Springer Science+Business Media B.V., Austin, Texas, USA, pp. 95–106.